On the Conflicting Estimations of Pigment Site Energies in Photosynthetic Complexes: A Case Study of the CP47 Complex

Tonu Reinot[1], Jinhai Chen[1], Adam Kell[1], Mahboobe Jassas[1], Kevin C. Robben[1], Valter Zazubovich[2] and Ryszard Jankowiak[1,3]

[1]Department of Chemistry, Kansas State University, Manhattan, KS, USA. [2]Department of Physics, Concordia University, Montreal, QC, Canada. [3]Department of Physics, Kansas State University, Manhattan, KS, USA.

ABSTRACT: We focus on problems with elucidation of site energies (E_0^n) for photosynthetic complexes (PSCs) in order to raise some genuine concern regarding the conflicting estimations propagating in the literature. As an example, we provide a stern assessment of the site energies extracted from fits to optical spectra of the widely studied CP47 antenna complex of photosystem II from spinach, though many general comments apply to other PSCs as well. Correct values of E_0^n for chlorophyll (Chl) a in CP47 are essential for understanding its excitonic structure, population dynamics, and excitation energy pathway(s). To demonstrate this, we present a case study where simultaneous fits of multiple spectra (absorption, emission, circular dichroism, and nonresonant hole-burned spectra) show that several sets of parameters can fit the spectra very well. Importantly, we show that variable emission maxima (690–695 nm) and sample-dependent bleaching in nonresonant hole-burning spectra reported in literature could be explained, assuming that many previously studied CP47 samples were a mixture of intact and destabilized proteins. It appears that the destabilized subpopulation of CP47 complexes could feature a weakened hydrogen bond between the 13^1-keto group of Chl29 and the PsbH protein subunit, though other possibilities cannot be entirely excluded, as discussed in this work. Possible implications of our findings are briefly discussed.

KEYWORDS: CP47, photosynthesis, redfield, simplex, Chl site energies

CITATION: Reinot et al. On the Conflicting Estimations of Pigment Site Energies in Photosynthetic Complexes: A Case Study of the CP47 Complex. *Analytical Chemistry Insights* 2016:11 35–48 doi:10.4137/ACI.S32151.

TYPE: Expert Review

RECEIVED: February 15, 2016. **RESUBMITTED:** April 10, 2016. **ACCEPTED FOR PUBLICATION:** April 26, 2016.

ACADEMIC EDITOR: Gabor Patonay, Editor in Chief

PEER REVIEW: Five peer reviewers contributed to the peer review report. Reviewers' reports totaled 2,012 words, excluding any confidential comments to the academic editor.

FUNDING: RJ acknowledges support from the Division of Chemical Sciences, Geosciences, and Biosciences, Office of Basic Energy Sciences of the U.S. Department of Energy through grant DE-SC0006678. VZ acknowledges support from NSERC. The authors confirm that the funder had no influence over the study design, content of the article, or selection of this journal.

COMPETING INTERESTS: Authors disclose no potential conflicts of interest.

CORRESPONDENCE: ryszard@ksu.edu

Paper subject to independent expert single-blind peer review. All editorial decisions made by independent academic editor. Upon submission manuscript was subject to anti-plagiarism scanning. Prior to publication all authors have given signed confirmation of agreement to article publication and compliance with all applicable ethical and legal requirements, including the accuracy of author and contributor information, disclosure of competing interests and funding sources, compliance with ethical requirements relating to human and animal study participants, and compliance with any copyright requirements of third parties. This journal is a member of the Committee on Publication Ethics (COPE).

Provenance: the authors were invited to submit this paper.

Published by Libertas Academica. Learn more about this journal.

Introduction

Photosynthetic complexes. Light-absorbing chromophores in various photosynthetic complexes (PSCs) initiate a highly complex series of processes.[1] The latter drives chemical reactions that support nearly all life on the Earth.[1] To understand the excitonic structure and dynamics of PSCs, it is essential to know: (i) pigment site energies (E_0^n), the transition energies in the absence of pigment–pigment interactions; (ii) intramolecular vibrational modes; (iii) interpigment couplings; and (iv) interactions between pigments and the protein environment, ie, electron–phonon (el–ph) coupling. Electronic coupling to phonon and intramolecular modes is characterized by the phonon and vibrational spectral densities, ie, $J_{ph}(\omega)$ and $J_{vib}(\omega)$, respectively.[2,3] While spectral densities can be measured experimentally[4–8] and interpigment coupling matrix elements can be calculated (assuming that X-ray structures are available) by several approaches,[9] the site energies are typically extracted from simultaneous fits of various experimental data.[7,10,11] Quantum chemical approaches can also be used,[9,12–15] but the calculated values have to be further optimized by fitting algorithms; however, the values obtained for structure-based calculations can aid in discarding unrealistic site energy sets obtained from the fitting algorithm. Conversely, the calculated site energies determined from fits of experimental results can test the accuracy of various quantum mechanical methods used in site energy calculations. The difficulties in finding real site energies are not surprising, as PSCs are very intricate biological systems.

Spectroscopic techniques often used in photosynthesis research. Widely used methods include high-resolution (laser-based) frequency-domain spectroscopies, ie, hole burning (HB) and fluorescence line narrowing (FLN),[16,17] single photosynthetic complex spectroscopy,[18,19] circular dichroism (CD) and linear dichroism (LD),[20] and circularly polarized luminescence (CPL).[21–24] Time-resolved techniques (eg, pump-probe[25–27] and two-dimensional electronic spectroscopies[28,29]) are also used and provide more information about the dynamics of PSCs.

Challenges facing determination of chromophore site energies in PSCs. Although many individual components of photosynthetic machinery are quite well understood, some questions remain unanswered.[30] The purpose of

this work is not to criticize the published site energies for various PSCs but rather to raise a genuine concern regarding the underlying reasons for conflicting estimations and accuracy of pigment site energies reported in many publications for the CP47 antenna. Therefore, we comment on the uncertainties that may affect the fitted E_0^n values of various chromophores. For example, sample purity (ie, the presence of contamination) and protein stability (ie, samples could consist of mixtures of intact and somewhat destabilized/damaged proteins). Furthermore, in low-temperature spectroscopy, high-fluence measurements may also modify optical spectra, changing absorption and emission spectra due to unaccounted HB. The latter problem is even more prominent in single photosynthetic complex spectroscopy studies where high-fluence light is routinely used to generate single-complex spectra (see discussions in Refs. 31 and 32). One also needs to be mindful of photochemistry, which can be either reversible or irreversible. For example, in bacterial reaction centers (RCs) (eg, *Rhodobacter sphaeroides* or *Rhodopseudomonas viridis*), the relatively weak probing light used to measure absorption spectra can not only significantly bleach the so-called P-band (due to very efficient charge separation) but also electrochromically shift the bands of accessory $BChl_L$ and $BChl_M$. Thus, these absorption measurements can significantly modify site energies, and as a result, optical spectra.[33]

One of the main obstacles in providing a unified description of the structure–function relationship in PSCs, protein energy landscapes, and *dynamics* of intact, wild-type, and mutated LH antennas is that various techniques are often applied to samples that show significantly different shapes of basic optical spectra, ie, absorption and emission spectra. The latter is a real limitation that raises questions regarding the relevance of pigment site energies extracted from different spectra (vide infra). Another important issue, as discussed in Refs. 3 and 33, is using a proper shape of $J_{ph}(\omega)$, which also affects the extracted site energies and population dynamics. For example, it is not clear: (i) whether an experimentally determined spectral density obtained via the delta FLN methodology, within the lowest energy state, is the same for all pigments; (ii) whether the el–ph coupling strength is sufficiently similar for all chromophores; (iii) to what extent inhomogeneous broadening (Γ_{inh}) varies from pigment to pigment; (iv) if the protein dielectric constant varies for different binding sites; and (v) how one should determine excitonic domains using a single coupling cutoff value. In fact, all of the above could depend on the protein-binding pocket. Thus, it is feasible to assume that a single solution based on modeling studies alone may not exist and a large number of experimental constraints (not available as of yet) are needed to narrow the possible choices.

Below, we present a case study of the aforementioned issues applied to the CP47 antenna by demonstrating nearly perfect simultaneous fits of multiple spectra with different sets of parameters, raising concerns about the parameters used to describe the excitonic structure of this important photosynthetic antenna complex. The key questions addressed are as follows: (i) why are there conflicting optical spectra reported in the literature for this antenna system? and (ii) is it possible to reconcile the different maxima and shapes of the reported fluorescence spectra? First, we note that this is a distinctly challenging protein to study, as CP47 is more difficult to separate from the photosystem II core complex (PSII-cc) than, for example, the accompanying CP43 antenna.[34,35] This is probably why somewhat different optical spectra have been reported over the years, which has led to disagreement about which spectra represent *intact* CP47 complexes and should they be used in modeling studies.[36–38] As a result, there is no agreement as to which chlorophyll (Chl) contribute to the lowest energy exciton state(s) and what their corresponding site energies are.[10,11,36]

Results and Discussion

Figure 1 shows the arrangement of CP47 Chls in relation to the RC chromophores. This antenna facilitates excitation energy transfer to the PSII RC.[11,25,39] Even though CP47 has been extensively studied over the years, the shape of various optical spectra of intact complexes (eg, absorption and emission spectra), extracted site energies (vide infra), and the resulting excitonic structure are still under debate. Typically, low-temperature steady-state absorption, emission, nonresonant HB, and room temperature (RT) CD and LD spectra of CP47 are used in modeling studies utilizing simple excitonic calculations[7] and Redfield simulations, taking lifetime

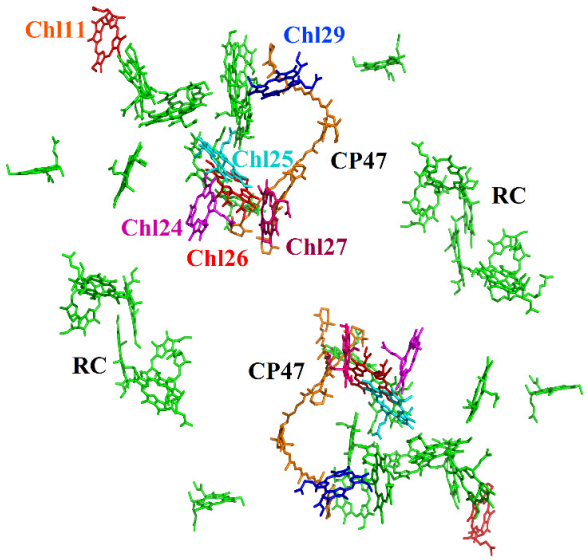

Figure 1. Arrangement of CP47 Chls in relation to the RC pigments within PSII-cc dimer based on the 1.9 Å resolution structure (PDB ID: 3WU2).[40] Each CP47 complex contains 16 Chls and 3 carotenoids (in orange). Pigments likely contributing to the lowest exciton states are separately colored and labeled (see text).

broadening effects into account.[10,11] In this study, we focus only on Redfield simulations for a straightforward comparison. Our modeling studies described below are based on the 1.9 Å resolution structure of the PSII core (PDB ID: 3WU2) from cyanobacteria.[40] While the experimental data are obtained for CP47 from spinach, it is believed that CP47 complexes are similar in PSII from all organisms. Unfortunately, no X-ray data for spinach PSII are available, and structure-based calculations by necessity are based on cyanobacterial structures.

Typical absorption, emission, and spectral densities used in modeling studies of CP47. Peak maxima varying from 690 to 695 nm in CP47 fluorescence spectra have been reported,[10,11,26,36,37,41–43] where the 695 nm band corresponds to intact CP47 complex.[36,37] Thus, the variable peak maxima suggest that complexes with blueshifted emission (near 690–693 nm) must be partly modified. This suggestion is consistent with the results obtained for intentionally damaged CP47 complexes (data not shown). To illustrate the discrepancies mentioned above, Figure 2A shows typical 5 K absorption and emission spectra for CP47 from the literature.[36] The emission spectrum in frame A is peaked at ~691 nm and has a full-width at half-maximum (FWHM) of 270 cm^{-1} (12.9 nm),[36] which is in general agreement with the previously published data (~260 cm^{-1}).[10,26] Notably, the emission maximum in frame B, for a carefully prepared and treated sample, peaks near 695 nm with the FWHM of just 195 cm^{-1}. The 695 nm emission is in agreement with the data obtained for PSII-cc, which is believed to contain intact CP47 proteins. This suggests, as argued in our previous articles,[36,37] that this sample represents the most intact CP47 complex, whereas typical CP47 spectra shown in frame A (and many 77 K spectra reported in Refs. 41–44) are representative of a mixture of intact and destabilized complexes.[36,37]

It has been suggested that the absence of ~695 nm emission,[38] or its decrease,[47,48] might be related to the absence of the PsbH protein subunit in the isolated CP47 complexes. However, it is possible that all CP47 complexes possess the PsbH subunit, and rather a subpopulation of complexes could have a weakened (or broken) hydrogen bond (H-bond) between one of the CP47 Chls and the amino acid residues of PsbH. For example, Thr5 of PsbH forms an H-bond with Chl29 of CP47.[38,49,50] If this H-bond is broken or weakened in a fraction of CP47 complexes, a blueshift of the Chl29 site energy should occur.[51] As a result, variable blueshifted emission spectra should be observed, in agreement with the experimental data. A similar mechanism involving weakened hydrogen bonds for other Chls could explain the absorption and emission spectra shown in Figure 2 (vide infra).

We emphasize again that only the redshifted emission near 695 nm (see Fig. 2B) is clearly observed in PSII membrane fragments[41,45,46] and PSII-cc from *Thermosynechococcus elongatus*,[39] which are considered to be intact preparations. Figure 3 shows 5 K PSII-cc emission spectra before and after HB (curves a and b, respectively), while the inset shows 77 K spectra of intact PSII-cc and CP47 (red curve). These data clearly indicate that absorption of the CP47 complex has experienced nonphotochemical HB at 5 K and that the 695 nm emission of CP47 is consistent with that observed for intact PSII-cc samples (for more details, see Ref. 39). Only data in Figure 2B are consistent with Figure 3.

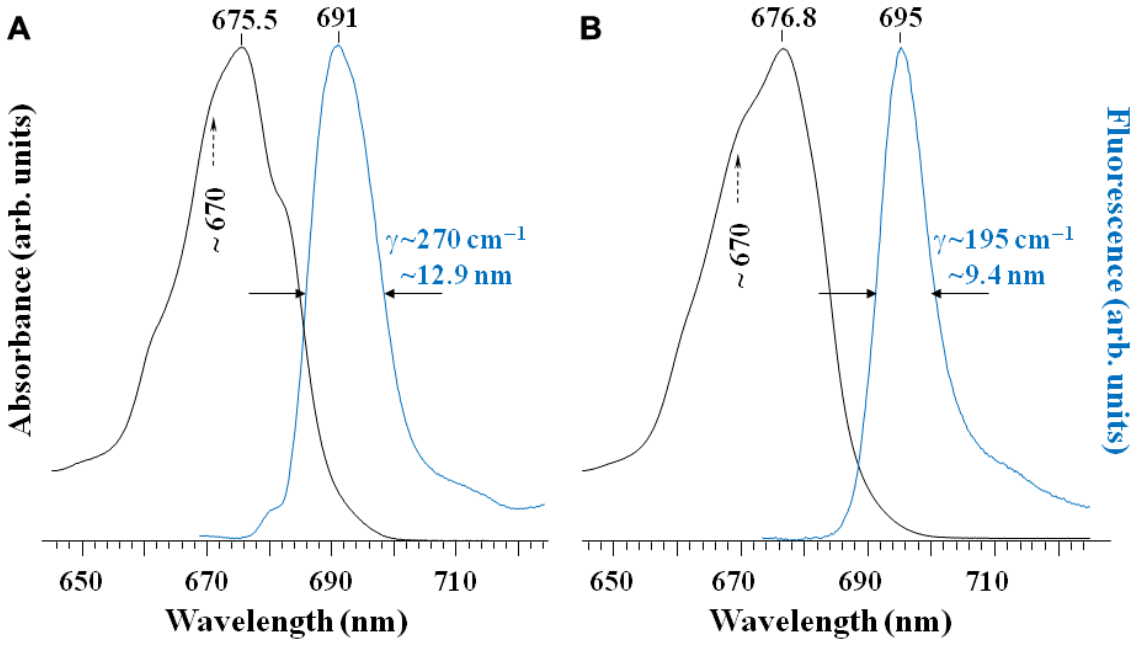

Figure 2. 5 K fluorescence and absorption spectra of the CP47 complex reported in Refs. 36 and 37. Spectra in frames **A** and **B** were measured for partly destabilized and intact samples from spinach.[36] Only frame **B** shows emission spectrum consistent with that observed in thylakoid membranes[41,45,46] and PSII-cc.[39] Reprinted with permission from Ref. 36. Copyright 2010 American Chemical Society.

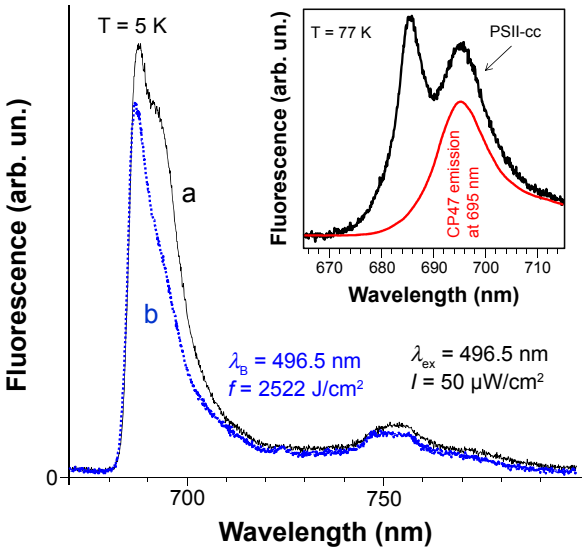

Figure 3. PSII-cc emission spectra of *T. elongatus* before (curve a) and after (curve b) bleaching of the lowest energy state of the CP47 complex responsible for the 695 nm emission at 5 K. λ_B = 496.5 nm and both spectra were obtained with λ_{ex} = 496.5 nm and I = 50 μW cm^{-2}. In the inset is the 77 K emission spectra obtained for PSII-cc from *T. elongatus* (black curve) and CP47 with a maximum at 695 nm (red curve).[37] Reprinted from Ref. 39 (Copyright Springer Science + Business Media Dordrecht 2015) with the permission of Springer.

Spectral densities. Additionally, we point out that different spectral densities, $J_{ph}(\omega)$, were used over the years to fit optical spectra of *various* PSCs—making an otherwise convincing assignment of site energies less tenable. The left frame in Figure 4 shows the single-site fluorescence spectrum calculated using a lognormal $J_1(\omega)$ compared with ΔFLN spectrum for the CP47 sample characterized by a 695 nm emission band at low temperatures. The right frame compares $\omega^2 J(\omega)$ (corresponding to the antisymmetric component of the Fourier–Laplace transform of the energy gap correlation function) for $J_1(\omega)$ (curve a), $J_2(\omega)$ (curve b), and the B777 $J(\omega)$ (curve c) from Refs. 10 and 11. $J_2(\omega)$ is a broader lognormal distribution than $J_1(\omega)$ and is used in modeling studies for higher energy pigments, as $J_1(\omega)$, measured for the lowest energy state, may not account for the expected fast exciton relaxation dynamics if used for all Chls. Note that $\omega^2 J(\omega)$ determines lifetime broadening effects and transition energy shifts. Thus, it is obvious that its shape will affect the extracted site energies. The B777 $J(\omega)$ (see curve c in Fig. 4), obtained from FLN data of the B777 subunit of LH1,[52] was used in several previous modeling studies of CP47.[10,11]

Modeling studies. Disorder is introduced into the diagonal matrix elements (ie, E_0^n) by a Monte Carlo approach with normal distributions centered at E_0^n (n labeling various pigments, ie, n = 1–16) and with FWHM representing Γ_{inh}, which can be site dependent or independent. Eigen decomposition of the interaction matrix provides eigen coefficients (c_n^M) and eigenvalues (ω_M). All 16 Chls are tested as the red-most pigment with E_0^n of 14,500 cm^{-1}, while other pigments are initially set at higher energies. E_0^n, Γ_{inh}, and phonon/vibrational S factors are used as free or fixed parameters (depending on the model) and are optimized simultaneously against the experimental spectra. Since it is not obvious that $J_{ph}(\omega)$ measured for pigments contributing to the lowest exciton state is the same for higher energy pigments, the effect of a broader $J_{ph}(\omega)$ shape

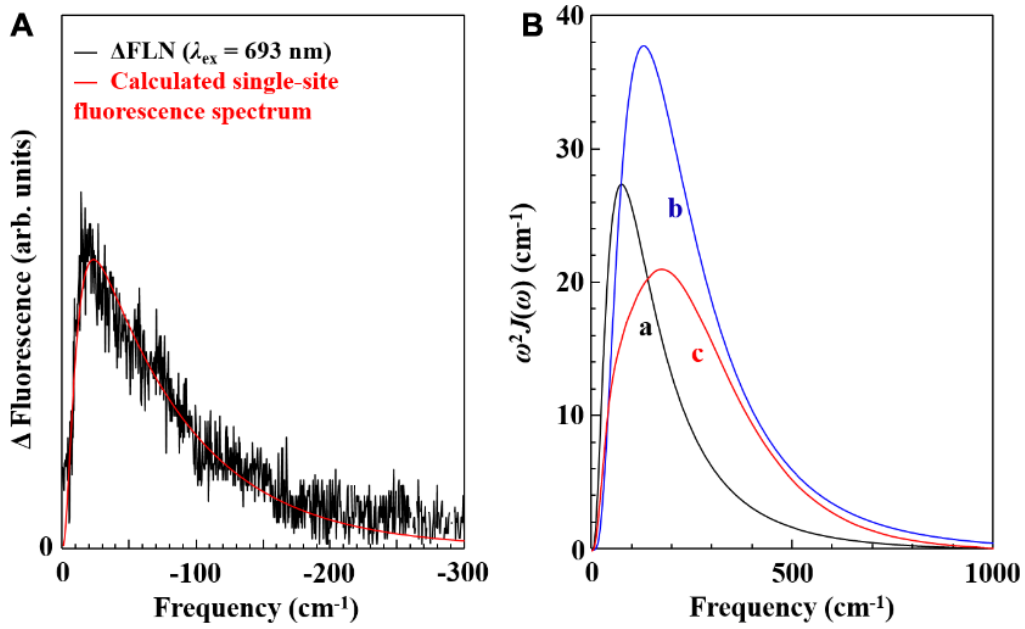

Figure 4. (**A**) Experimental ΔFLN spectrum fit using a lognormal distribution for $J(\omega)$. ω_c = 40 cm^{-1} and σ = 0.8, where ω_c and σ are the cutoff frequency and standard deviation, respectively, and the Huang–Rhys factor (S) is 1.0. (**B**) Comparison of $\omega^2 J(\omega)$ for $J_1(\omega)$ from left frame (curve a), $J_2(\omega)$ (a lognormal distribution with ω_c = 80 cm^{-1}, σ = 0.7, and S = 0.65; curve b), and the B777 $J(\omega)$ with S = 0.6 (curve c).[52]

(see Fig. 4B) with a different S factor and/or variable Γ_{inh} is also tested for comparison. Calculated spectra are modeled using a newly developed algorithm that can simultaneously fit several experimental spectra at different temperatures, providing constraints on the pigment site energies of interest.

To address the excitonic structure of the CP47 protein, we begin below with the best fits of our experimental steady-state absorption/emission (from Fig. 2B),[36] RT CD,[53] and our nonresonant HB spectrum (5 K, λ_B = 496.5 nm).[36] All samples were prepared as described previously.[36,37] As argued before,[36,37] these data, in our opinion, correspond to the most intact CP47 complexes of PSII from spinach studied in our laboratory over the years. In simulations, we used a non-Markovian reduced density matrix theory[52] with a Nelder–Mead simplex algorithm for parameter optimization.[54] Errors between optimized fits and experimental spectra are reported as the root-mean-square deviation. The Chls within CP47 were divided into the same domains of coupled Chls as in Ref. 11, with coupling matrix elements calculated by the TrEsp method developed by Madjet et al.[55] A coupling cutoff (V_c) of 40 cm^{-1} is used to split the Hamiltonian into the five exciton domains of Ref. 11. For brevity, we discuss only the calculated spectra, exciton composition (focusing on the lowest energy exciton states), and the extracted site energies.

Several different models are considered below. In Model A, we use the experimentally determined $J_{ph}(\omega)$ for all pigments and allow Γ_{inh} to vary independently for all Chls. Herein, we use V_{mn} values calculated with the TrEsp method.[55] The best fits were obtained for three sets of parameters in Model A, which are referred to below as Models 24A, 26A, and 29A (where the number identifies the lowest energy Chl). The results for Models 24A, 26A, and 29A are shown in Figures 5–7, respectively. This is consistent with our previous extensive searches for realistic low-energy pigments.[7] That is, previously published articles suggested that Chl26[7] or Chl29[10,11] are the best candidates to contribute mostly to the lowest energy state, although *different* shapes of emission/absorption spectra, spectral densities, and levels of theory were used in modeling studies. Left panels in Figures 5–7 show calculated curves as solid lines, and experimental curves are filled. Right panels in Figures 5–7 show the respective first three excitonic states (top) and the major pigment contributions (right bottom panels) to the respective lowest energy ($\alpha = 1$) state.

Figure 5 presents Model 24A, where the lowest energy pigment, Chl24, has $E_0^n/\Gamma_{inh} = 14,485/152\,\text{cm}^{-1}$. Herein, Chl24, Chl26, and Chl29 contribute to the lowest (α = 1) exciton states 92%, 2%, and 2%, respectively. A virtually perfect fit of the ~695 nm emission spectrum was obtained. Figures 6 and 7 show fits to the same experimental spectra starting from different site energies, assuming that either Chl26 or Chl29, respectively, mostly contribute to the lowest energy trap (as reported in Refs. 7, 10, and 11). Again very good fits can be obtained; in these two cases, the lowest energy chromophores are characterized by E_0^n/Γ_{inh} of 14,501/161 and 14,484/146 cm^{-1}, respectively. All fit parameters (including E_0^n and Γ_{inh} of all Chls) are summarized in Tables 1 and 2, while the previously reported values from Refs. 10 and 11 are summarized for comparison in Supplementary Table 1.

Recall that in fitting simultaneously all four spectra in Models 24A, 26A, and 29A, we assume that all Chls could have somewhat different Γ_{inh}. The fits of the same four experimental spectra as those shown in Figures 5–7, assuming *the same* Γ_{inh} for all pigments except the lowest

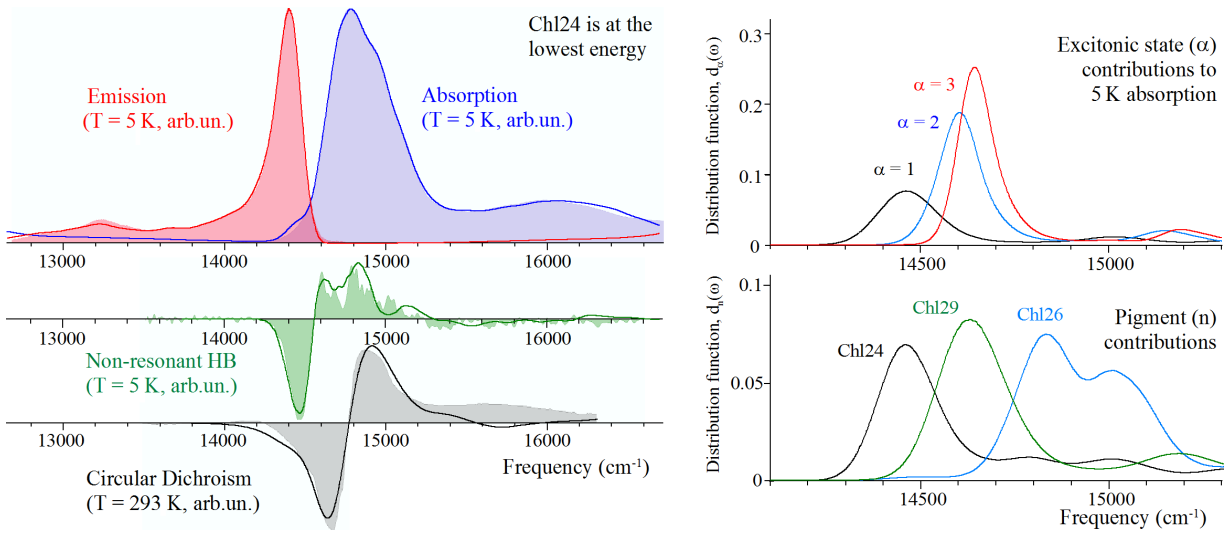

Figure 5. Model 24A. Left: best simultaneous fits (lines) of 5 K absorption (blue), emission (red), and low-fluence nonresonant HB (green) spectra compared to experiment (filled curves). Gray curves are experimental and calculated RT CD spectra. Lowest energy Chl24 and Chl29 have E_0^n/Γ_{inh} of 14,485/152 and 14,710/224 cm^{-1}, respectively. Right: contributions to 5 K absorption of the three lowest energy exciton states (top) and the three pigments that contribute most to the α = 1 exciton state (bottom). Fitting error = 1.15 × 10^{-3}.

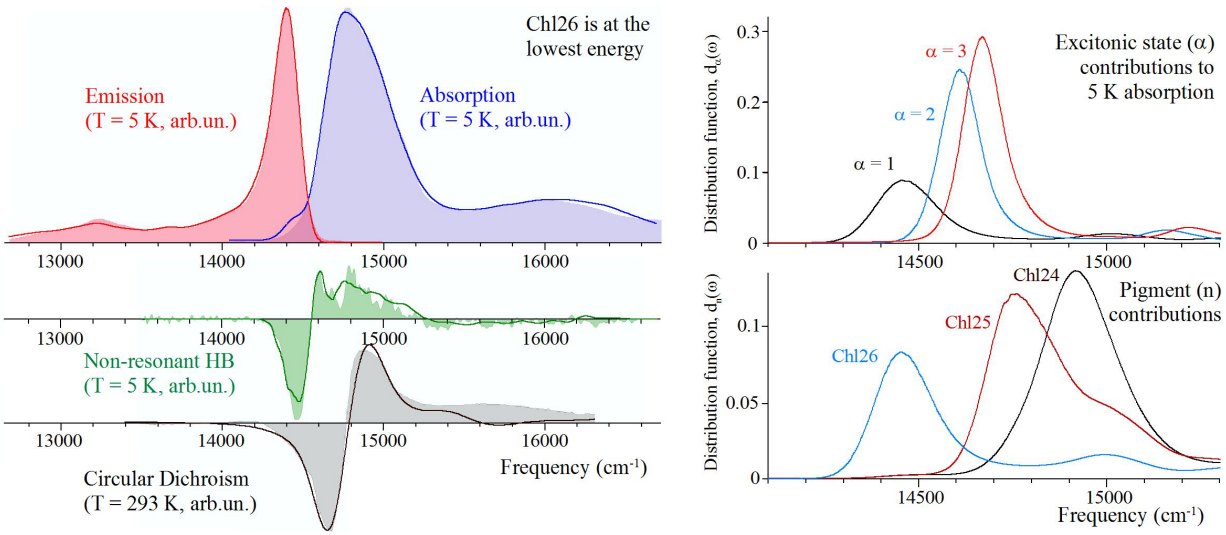

Figure 6. Model 26A. The same experimental data as in Figure 5. Lowest energy Chl26 and Chl29 have E_0^n/Γ_{inh} of 14,501/161 and 14,662/187 cm^{-1}, respectively. Chl26, Chl24, and Chl29 contribute 91%, 2%, and 2% to the lowest energy (α = 1) state, respectively. Fitting error = 1.19×10^{-3}.

energy one (referred to as Model B), also provide very good fits when Chl24 (Model 24B), Chl26 (Model 26B), or Chl29 (Model 29B) has the lowest site energy; that is, in Model B, we assume that Γ_{inh} is site independent for all but the lowest energy Chl, which is constrained by the width of the fluorescence and HB spectra. The best fits in Models 24B, 26B, and 29B were obtained with Γ_{inh} of 221, 218, and 241 cm^{-1}, respectively, for all high-energy Chls. The resulting fits are shown in Supplementary Figures 1–3.

Although the fits for Model B are good, as expected, the site energy differences between Models A and B are on the order of 1 nm (see Table 1 and the Supplementary File). However, the lack of detailed information on Γ_{inh} complicates the analysis, as multiple sets of parameters provide good fits to experimental spectra. Thus, we do not assert that the site energies shown in Table 1 are perfect. However, a comparison between site energies obtained for *variable* and the *same* Γ_{inh} for all but one pigment (vide supra) introduced relatively small changes. For example, the average difference between the E_0^n between Models 29A and 29B is only 0.5 nm, though the difference ranges from values –1.9 to 0.9 nm. Variations for other models are also listed at the bottom of Table 1.

Next, one could test whether $J_1(\omega)$ (curve a in Fig. 4) is a proper choice for all Chls. To test this, Model 29C assumes two $J_{ph}(\omega)$, curves a and b from Figure 4, ie, $J_1(\omega)$ measured

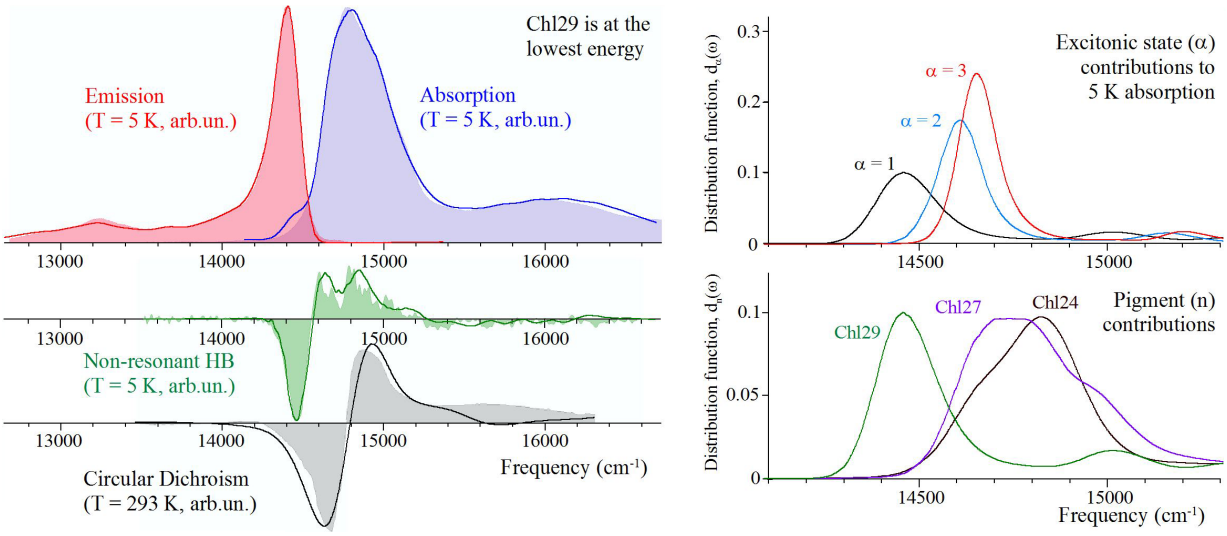

Figure 7. Model 29A. The same experimental data as in Figures 5 and 6. Lowest energy Chl29 and Chl24 have E_0^n/Γ_{inh} of 14,484/146 and 14,759/250 cm^{-1}, respectively. Chl29, Chl24, and Chl27 contribute 94%, 2%, and 1% to the lowest energy (α = 1) state, respectively. Fitting error = 1.34×10^{-3}.

Table 1. Site energies for Models 24A/B, 26A/B, and 29A/B/C (see text).

CHL	24A	24B	Δ24 (A–B)	26A	26B	Δ26 (A–B)	29A	29B	Δ29 (A–B)	29C	Δ29 (A–C)
11	678.7 (3)	678.2 (3)	0.5	676.2 (4)	676.2 (4)	0.0	674.8 (4)	674.7	0.1	672.9	1.9
12	672.2	673.6	–1.4	675.7	676.3 (3)	–0.7	668.4	668.3	0.0	671.9	–3.5
13	675.9 (4)	676.0 (3)	–0.1	673.4	672.8	0.6	673.2	672.3	0.9	671.5	1.7
14	661.8	660.3	1.6	670.7	671.3	–0.6	669.8	669.1	0.7	667.2	2.6
15	664.8	664.6	0.2	676.4 (3)	676.1	0.3	674.7	673.8	0.9	672.5	2.2
16	674.0	675.5	–1.5	676.1	675.9	0.2	672.6	674.0	–1.4	674.1	–1.5
17	669.0	670.2	–1.2	663.6	663.8	–0.2	663.5	662.7	0.7	662.9	0.6
21	675.3	674.7	0.5	673.2	673.5	–0.4	674.6	675.2 (4)	–0.6	673.2	1.4
22	665.3	664.8	0.5	662.6	662.0	0.7	661.5	661.2	0.3	662.9	–1.4
23	665.2	665.2	–0.1	665.9	665.4	0.5	667.9	667.8	0.1	664.7	3.1
24	690.4 (1)	690.4 (1)	0.0	670.0	669.6	0.4	677.6 (2)	677.7 (2)	–0.1	677.9 (2)	–0.3
25	673.5	673.4	0.2	671.4	671.7	–0.3	671.9	671.8	0.0	670.2	1.7
26	668.1	668.8	–0.8	689.6 (1)	689.6 (1)	0.0	673.5	675.4 (3)	–1.9	675.6 (3)	–2.2
27	672.6	672.5	0.1	668.4	668.5	–0.2	675.1 (3)	674.8	0.3	674.3 (4)	0.8
28	666.7	665.9	0.8	662.7	662.6	0.1	663.0	662.8	0.2	661.4	1.6
29	679.8 (2)	678.9 (2)	1.0	677.4 (2)	677.3 (2)	0.2	690.4 (1)	690.4 (1)	0.0	690.3 (1)	0.1

Notes: Pigments are labeled according to nomenclature of Loll et al.[49] Δ shows the difference between site energies of various models. The red numbers in parentheses indicate energy ordering of the four lowest energy Chls for easy comparison. All values are in units of nanometer.

experimentally for the lowest state ($\omega_c = 40$ cm^{-1}, $\sigma = 0.8$, and $S = 1$) and $J_2(\omega)$ with $\omega_c = 80$ cm^{-1}, $\sigma = 0.7$, and $S = 0.65$ for higher energy pigments; that is, $J_2(\omega)$ is used for all pigments except Chl29. As expected, addition of the broader $J_2(\omega)$ somewhat compensates for Γ_{inh}, on average, down from 241 to 216 cm^{-1} (for Model 29C). However, we emphasize again that all spectra can be simultaneously well fitted with different sets of site energies, as shown in Table 1. The fits for Model 29C are shown in Figure 8.

Table 2. Γ_{inh} (FWHM) for Models 24A, 26A, and 29A.

CHL	MODEL 24A	MODEL 26A	MODEL 29A
11	198	234	253
12	273	234	258
13	229	231	230
14	230	220	264
15	249	225	232
16	248	176	263
17	235	216	255
21	154	240	244
22	236	219	256
23	238	223	262
24	152	227	250
25	228	221	255
26	266	**153**	273
27	196	208	231
28	223	199	262
29	224	169	146

Note: All values are in units of per centimeter.

Finally, there are also various methods for calculating the interaction between pigment transition dipoles.[9] Although the TrEsp method has been used in both this work and Ref. 10, the more complicated Poisson–TrEsp method, accounting for electrostatic potential of the protein environment, was used to calculate the coupling constants of Ref. 11. On average, Poisson–TrEsp produces values ~0.7 smaller than the standard TrEsp method (see Supplementary Tables 2 and 3). Note that very good fits can also be obtained for the above models (24A/B, 26A/B, and 29A/B) using the smaller coupling constants from Ref. 11, ie, calculated with the Poisson–TrEsp method and $V_c = 30$ cm^{-1}. Thus, the differences between TrEsp and Poisson–TrEsp are not critical for providing good fits of optical spectra. For comparison, Figure 9 shows optimized fits of Model 29C using the Poisson–TrEsp values[11] (Model 29CP), as given in Supplementary Table 3. For brevity, we only mention that similar quality fits can be obtained for models in which Chl24 and Chl26 are the main contributors to the lowest energy state.

The data discussed above, as well as data shown in Supplementary Figures 1–3, show that multiple sets of Chl site energies can fit absorption, emission, CD, and nonresonant HB spectra. However, the values of elucidated site energies somewhat depend on assumptions regarding Γ_{inh} and shapes of $J_{ph}(\omega)$. Interestingly, taking mutational data into account,[47,48] one could suggest that Chl29 might indeed be the pigment of choice, as briefly discussed below, but one still cannot exclude that Chl24 and Chl26 are the lowest

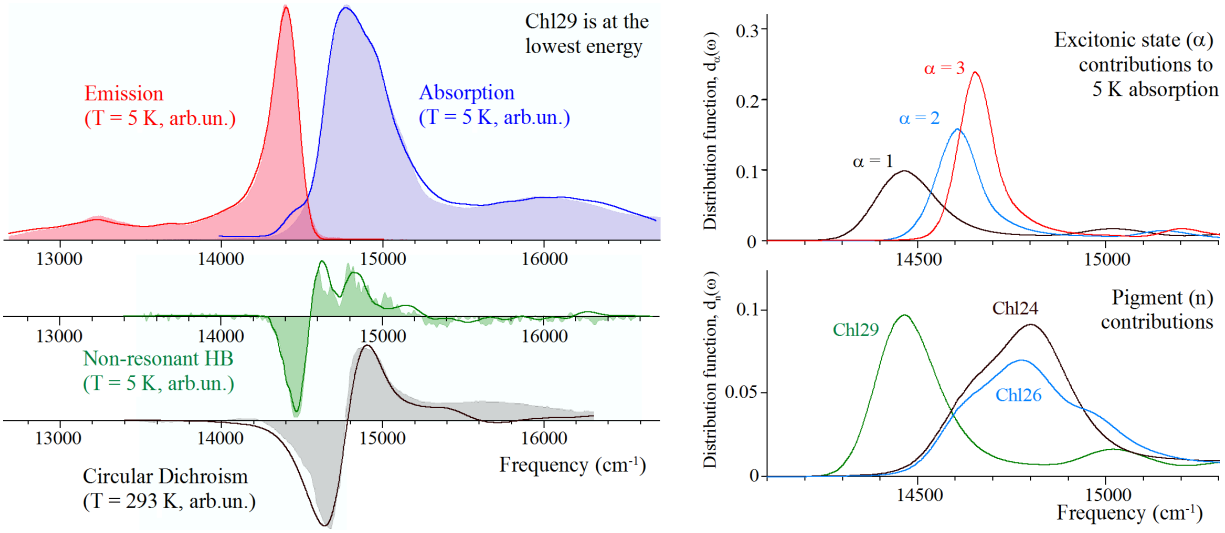

Figure 8. Model 29C. Lowest energy Chl29 and Chl24 have E_0^n/Γ_{inh} of 14,486/147 and 14,751/227 cm^{-1}, respectively. Chl29, Chl24, and Chl26 contribute 96%, 2%, and 1% to the lowest energy (α = 1) state, respectively. The el–ph coupling of Chl29 is described by $J_1(\omega)$, with all other Chls described by $J_2(\omega)$. Fitting error = 1.28×10^{-3}.

energy pigments. Thus, the quality of the fits (which appear to be very good for all models), even when multiple spectra are fitted simultaneously, does not guarantee a unique outcome, as a number of parameters discussed above are not well defined.

Hydrogen bonding and mutational studies in CP47. Recent experiments, where spectroscopic studies were performed on CP47 assembly modules containing or lacking the PsbH protein,[38] shed more light on the spectral differences reported in the literature for CP47 complexes.[26,36,37,41,42] An essential role of PsbH in the origin of the PSII red emission has been recently demonstrated.[38] The authors argued that based on the crystal structure,[40] PsbH directly interacts with Chl29 of CP47 through an H-bond between Thr5 and the Chl 13^1-keto group, which could be responsible for the red fluorescence state of CP47. These ideas were also previously discussed in Refs. 7 and 50. Now, if Chl29 is indeed the lowest energy pigment, as also proposed in Refs. 10, 11, 47, and 48, the stronger or weaker H-bond (due to protein destabilization) between Thr5 of the PsbH subunit and Chl29 (at least in a subpopulation of CP47 complexes) could explain the variable emission spectra reported in the literature. We test below whether or not it is feasible to assume that low-temperature spectra (5–77 K) reported and modeled in the past[10,11,56] could,

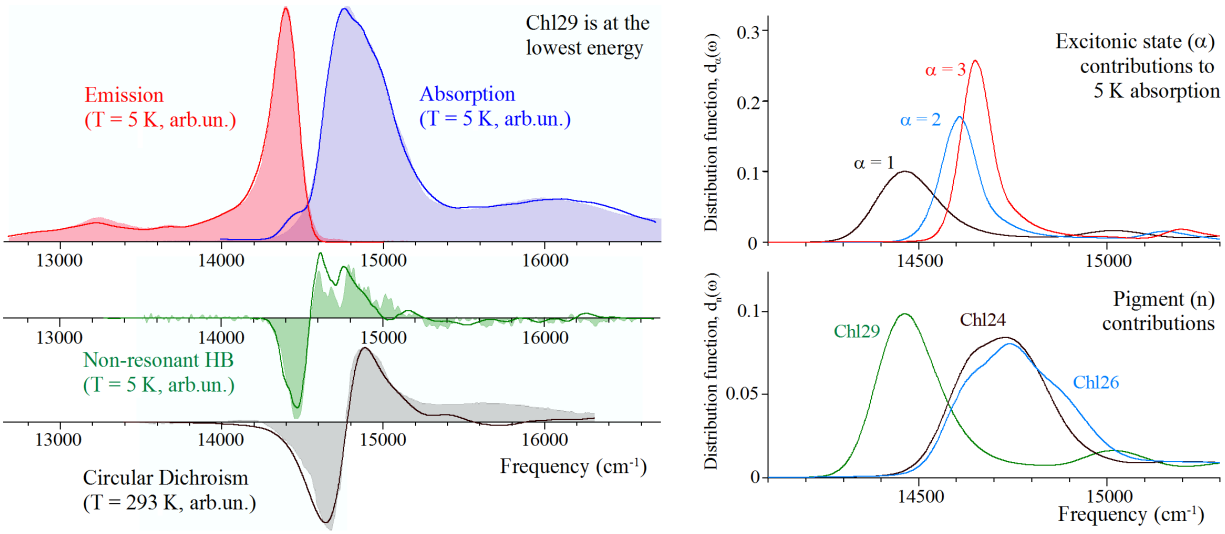

Figure 9. Model 29CP. Lowest energy Chl29 and Chl24 have E_0^n/Γ_{inh} of 14,486/147 and 14,721/188 cm^{-1}, respectively. Chl29, Chl24, and Chl26 contribute 97%, 2%, and 1% to the lowest energy (α = 1) state, respectively. Poisson–TrEsp coupling constants.[11] The el–ph coupling of Chl29 is described by $J_1(\omega)$, with all other Chls described by $J_2(\omega)$. Fitting error = 1.35×10^{-3}.

as suggested by us in Refs. 36 and 37, correspond to mixtures of intact and destabilized complexes.

Do the typically reported and modeled fluorescence spectra with FWHM of ~260–270 cm^{-1} correspond to a mixture of intact and destabilized CP47 complexes?. To test this suggestion, we use the parameters obtained from the fit of four optical spectra shown in Figure 8 with one exception; the site energy of Chl29 is shifted to higher energy, assuming that in samples with a contribution from destabilized proteins the H-bond with PsbH could be broken or significantly weakened. The latter is very feasible, though other minor changes could also occur. For example, de Weerd et al[42] observed the 1633 cm^{-1} mode in FLN spectra, indicative of an extremely strong H-bond between the 13^1-carbonyl group and the protein, which (at least in a subpopulation of complexes) could produce the redshift of one of the pigments contributing to the lowest energy state. In our 2010 article,[7] we questioned this interpretation, as in 2004 the above assignment was reversed by the same group,[44] as they did not find any strong evidence for a 1633 cm^{-1} mode. However, it is very likely that both sets of experimental data were correct, but the experiments were done on more intact and less intact CP47 samples. This, in turn, would suggest that CP47 samples can be a mixture of subpopulations in which the H-bond from the PsbH subunit to Chl29 (or other low-energy pigment) is strong or significantly weakened, though other minor changes to site energies of other pigments cannot be entirely excluded.

The data for a mixture of intact/destabilized CP47 complexes (with Chl29 being the lowest energy pigment in both subpopulations) are shown in Figure 10. The top spectra are identical to those shown in Figure 8 (for intact CP47, Model 29C) for easy comparison of shifts. The lower two panels are for the mixture of intact/destabilized sample (Model 29CM, where M indicates a mixture model). The CD spectrum is not shown in Figure 10, as the calculated spectrum is nearly identical to that shown in Figure 8 for the intact CP47 complex.

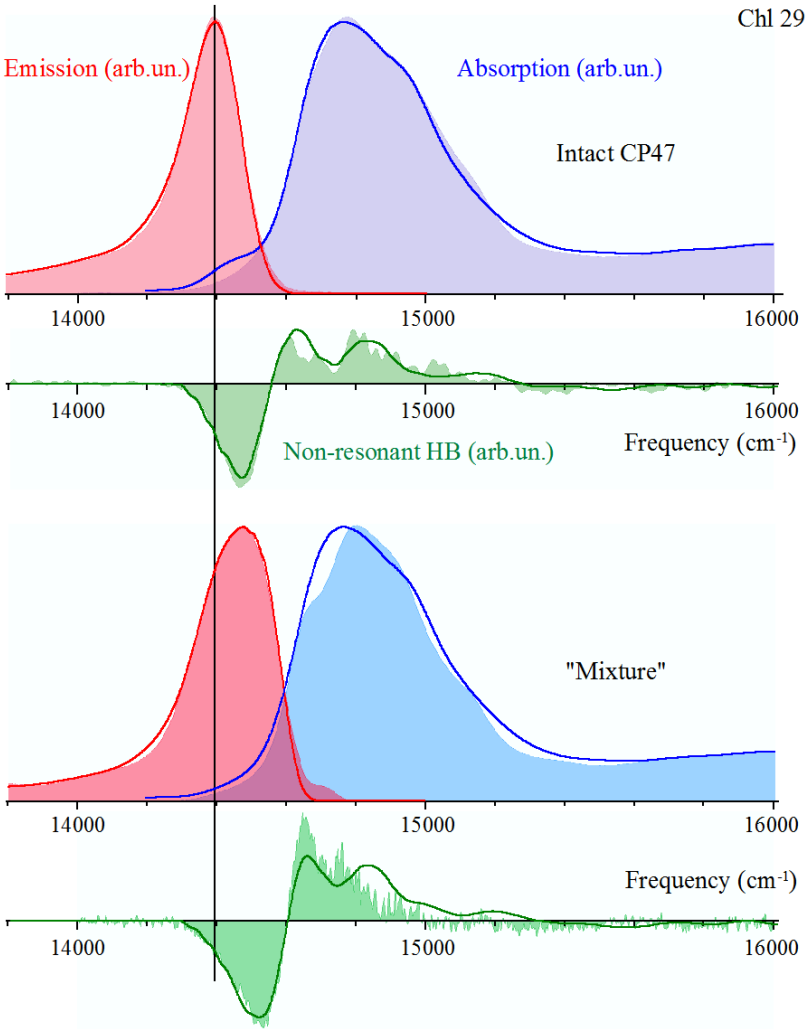

Figure 10. Filled spectra in the top and bottom frames are the experimental absorption, emission, and HB spectra for intact CP47 (Fig. 2B) and intact/destabilized CP47 complexes (Fig. 2A), respectively. All calculated spectra for Models 29C (top) and 29CM (bottom) are given by solid lines. The three spectra in the bottom panel can be well described, assuming a mixture of intact/destabilized (40%/60%) proteins. The only difference between intact and destabilized subpopulations is the site energy of Chl29 (see text).

Figure 10, which shows reasonable fits of the often reported spectra without any optimization, reemphasizes our previous conclusion that the broad (FWHM ~260–270 cm^{-1}) and blueshifted fluorescence spectra may indeed correspond to a mixture of intact and destabilized complexes; that is, all what was required to obtain good fits in Figure 10 was a 113 cm^{-1} shift of the site energy of Chl29 for the destabilized subpopulation and assuming at the same time a 40%/60% mixture of intact/destabilized contributions. Note that applying the optimization algorithm for site energies of higher energy Chls would improve the fits of absorption and HB spectra (data not shown). Of course, a different composition of intact and destabilized proteins will change the resulting emission spectrum in agreement with other experimental data, where often the maxima (for partly destabilized CP47 complexes) were reported to lie between 690 and 693 nm.[36,37,39] That is, samples with emission near 690 nm would contain mostly destabilized complexes (data not shown for brevity). Interestingly, fits similar to those shown in Figure 10 can also be obtained for Models 29AM and 29BM, as illustrated in Supplementary Figures 4 and 5.

Furthermore, at this point, it cannot be excluded that Chl26 could be the lowest energy Chl. In this case, one would have to assume that a putative H-bond between His9 of CP47 and the ester group of Chl26 exists and could be significantly weakened due to protein conformational changes. A similar scenario could also be feasible assuming that Chl24 contributes mostly to the lowest energy state, with a putative H-bond of the Chl24 ester group with either Trp468 or His9 of CP47 (in the latter case, based on Ref. 50, this could be an H-bond from the N_δ-atom). Data for the abovementioned scenarios involving Chl24 and Chl26 as the lowest energy pigments, though not shown for brevity, could also fit all the spectra in question. Although the *mixture models* with Chl26 or Chl24 as the lowest energy pigments could also be consistent with experimental data, they should be interpreted cautiously, as no strong H-bonds were found for these pigments in the structures in the studies by Loll et al[49] and Guskov et al.[57] Thus, there are no authoritative experimental or simulation data to provide just one solution for the lowest energy pigment(s), although based on mutational studies[47,48] it is likely that the best candidate for the lowest energy pigment could be Chl29. However, the lowest energy state of the modified subpopulations maybe localized on different pigments than the intact subpopulation, which could provide the abovementioned weakly positive CD signal at ~690 nm. Importantly, our simulation results clearly support our earlier suggestion that many previously reported optical spectra and their simulation data were obtained for mixtures of intact and destabilized proteins, questioning the validity of parameters reported in the literature.[7,10,11]

Returning to Figure 10, we note that shifting the site energy of Chl29 in Model 29CM (see above), or Models 29AM and 29BM (see Supplementary Figs. 4 and 5), leads to very small changes in the absorption and CD spectra, while significant changes occur in fluorescence and HB spectra, in very good agreement with experimental data.[36] Thus, our data provide more insight into possible composition of previously published fluorescence spectra (with maxima between 690 and 693 nm),[36,47,58] which revealed variable contributions from ~695 nm emission,[36,37] as well as of HB spectra. The mixture model is consistent with the measured fluorescence spectra and the observed (sample-dependent) shift in the nonresonant HB spectra and supports our previous conclusions.[36] This is why the width (FWHM) of various steady-state 77 K fluorescence spectra reported in the literature also varied from 16 to 24 nm, while the FWHM of fluorescence spectrum of intact CP47 complex at 77 K is only 12 nm.[36,37] In general, the FWHM of various ~5 K emission spectra are by a factor of ~1.3–1.7 larger than our emission spectrum obtained for the intact sample, which peaks at 694.8 nm and has a width of ~9.5 nm.[36,37] We hasten to add that the temperature dependence of various emission spectra can also be explained by our mixture model, but the results will be reported elsewhere.

Finally, we comment on parameters elucidated in Refs. 10 and 11 from the fits of 77 K spectra. Figure 11 shows calculated spectra using all parameters of Ref. 11, with Chl29 as the lowest energy Chl (that is, V_{nm}, $J_{ph}(\omega)$, S, E_0^n, and Γ_{inh}) compared with experimental data of Figure 2, as well as the corresponding HB spectra[36] and the RT CD spectrum.[53] Experimental data are shown in black, while calculated curves are shown in red. Note that the parameter set was optimized not to our experimental data shown in Ref. 36, but to various spectra taken from the literature.[26,42,53] It is obvious that parameters reported in Refs. 10 and 11 do not fit spectra shown in Figure 2, although the fit to CD is reasonable as this spectrum was also included in fits reported in Ref. 11. We admit that comparison of calculated parameters obtained from fits of different experimental spectra does not provide any insight, though it reveals again that samples of variable intact/destabilized composition were studied by various laboratories. This is also supported by the fact that parameters set from Refs. 10 and 11 do not fit emission spectra reported in Ref. 42 (not shown for brevity). Clearly, the results of this work have shown that until the shapes of standard spectra for the intact CP47 complex are established, spectral densities, inhomogeneous disorder, etc. are further constrained by experimental data, and ambiguous results can be obtained, in agreement with the main conclusions of this work.

Possible implications of our findings on the structure–function relationship of Chls in the CP47 complex. In light of the data presented above, we think that the analysis of the structure–function relationship in CP47 must await further work and confirmation of our mixture model(s). We still believe that even if Chl29 is the lowest energy pigment (with a localized excited state) it may not be important for excitation energy transfer to the RC. That is, Chl29 (in proximity to Car_{D2} and $ChlZ_{D2}$) could dissipate excess energy under

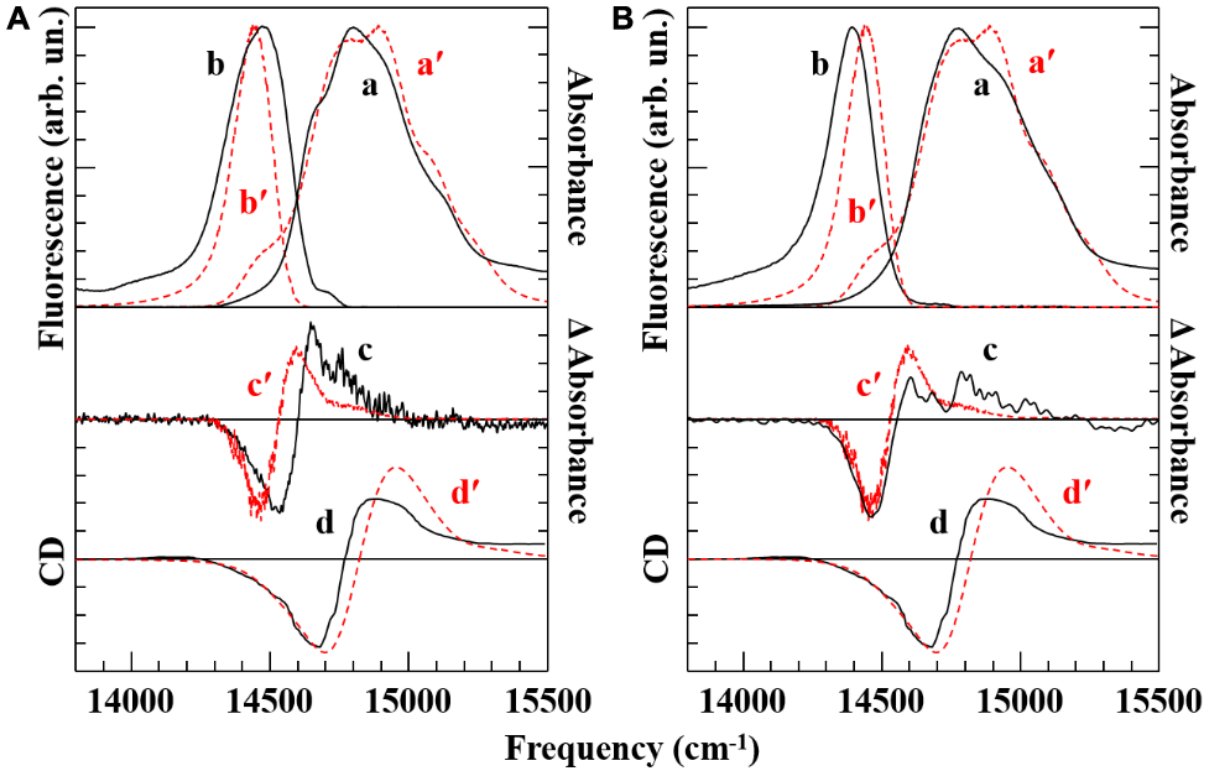

Figure 11. Experimental (black) and simulated (red) 5 K absorption (a/a′), fluorescence (b/b′), nonresonant HB (c/c′), and RT CD (d/d′) spectra. (**A**) and (**B**) correspond to the experimental spectra of Figure 2A and B, respectively (for details, see Ref. 36). The CD spectrum is the same for both frames.[53] The red curves are calculated using the parameters of Ref. 11 (see Supplementary Table 3 and text in the Supplementary File) and are the same in both frames.

conditions of high light intensity.[11] In the case where Chl24 or Chl26, located in the vicinity of the RC, contribute mostly to the lowest energy state, they could efficiently transfer energy to the RC. Of course, the assignment of low-energy pigments and the connection of these low-temperature assignments to function in vivo will depend on the shape of the low-temperature spectra being fit.

Concluding Remarks

In light of the difficulties and issues surrounding the extraction of pigment site energies discussed in this work, we believe that more insight into possible sets of site energies for the most intact and intact/destabilized CP47 samples was provided via computerized optimization cycles while simultaneously fitting absorption, emission, CD, and HB spectra. The assignment of site energies differs significantly from those reported recently by Shibata et al[11] for CP47 obtained by modeling 77 K spectra,[26,42] highlighting the complications involved in comparing the results from various modeling studies, especially, when different types of spectra are simulated using different $J_{ph}(\omega)$. Although, as shown above, assigning the lowest site energy to Chl24, Chl26, or Chl29 can fit the data very well, including both intact and mixtures of intact/destabilized complexes. Although it is likely (considering all mutagenesis data)[47,48] that Chl29, with an H-bond to the PsbH subunit, might be the best candidate as the major contributor to the lowest energy trap in intact CP47 complex, other assignments (eg, with Chl24 or Chl26 as the lowest energy pigments) cannot be entirely excluded. Very recent modeling of fluorescence kinetics of PSII in Ref. 56 also suggested that assigning Chl26 as the reddest absorbing Chl cannot be entirely excluded.

We conclude that spectra simulated in Refs. 10 and 11, as well as many spectra reported in the literature, likely correspond to a mixture of intact and destabilized complexes, where a H-bond between one of the Chls and the protein environment could be altered, though other reasons for the changes in Chl site energies cannot be excluded at this time, such as Chl conformations and the presence of nearby polarizable molecules. Thus, if Chl29 is indeed the lowest energy pigment, then the H-bond between its 13^1-keto group and Thr5 of PsbH could be broken or weakened, as indicated by very good fits of spectra corresponding to a mixture of intact/destabilized complexes (Fig. 10 and Supplementary Figs. 5 and 6).

In addition, it must be confirmed that the extremely weak positive CD spectrum near 692 nm observed in PSII core from spinach (at low-T)[59] is also observed in isolated, intact CP47 complexes. The latter is critically important as none of the site energies reported so far in the literature,[10,11] as well as parameters reported in this article (though excellent fits were obtained while simultaneously fitting multiple spectra), could reveal a positive CD peak near 692 nm within

the 5–300 K temperature range. If the lowest exciton state in CP47 is delocalized, the CD signal should be strong. Thus, more reliable low-T CD spectra are needed to address the nature of the low-energy excited state(s) in the CP47 complex. Herein, CPL, successfully obtained recently for the CP43 protein complex,[24] could also provide some insight into the composition of the lowest exciton state in the CP47 antenna. Thus, more experimental constraints are needed to reduce the variability in the reported Chl site energies and/or reveal new sets of parameters if necessary. In particular, the uncertainties for higher energy pigments are much larger, which in turn could affect the energy transfer rates/pathways. A final set of parameters must be able to describe all frequency- and time-domain data generated for the same well-characterized, intact protein complexes, and to the best of our knowledge, this has not been done as of yet. Our preliminary simulation data indicate that a different composition of the lowest exciton state might be necessary to describe positive CD bands near 692 nm. However, the latter must be demonstrated for intact isolated complexes, whose spectra are shown in Figure 2B.

Finally, more efforts are needed to theoretically explore spectral densities for pigments residing in different protein environments.[60–62] Furthermore, efforts should be made to determine if $J_{ph}(\omega)$ shapes could be elucidated from measurements of the average lifetimes of high-energy exciton states. The latter, if possible, would definitely improve the theoretical description of various linear and nonlinear optical spectra of many PSCs. This is very important, as small differences in the shape of $J_{ph}(\omega)$ (in particular, the high-frequency spectral region) can lead to large changes in exciton relaxation. Therefore, $J_{ph}(\omega)$ should be measured for each pigment–protein complex of interest. Finally, we emphasize that $J_{ph}(\omega)$, via ΔFLN or ΔHB spectroscopies, reveal spectral density and el–ph coupling parameters only for pigments contributing to the lowest energy exciton state.

In summary, our findings for the spectra reported in this article can be stated as follows: (i) the 695 nm emission band (with FWHM ~195 cm^{-1}) is the likely emission of intact CP47 at both 5 and 77 K, as such emission is also observable at both temperatures in PSII-cc[39,41] and thylakoid membranes;[41,45,46] (ii) blueshifted emission often observed near 690–693 nm must contain subpopulations of intact and destabilized complexes, and thus, an emission band with FWHM ~260–270 cm^{-1} (at ~5 K) peaking at 690–693 nm likely indicates a mixture of intact and destabilized CP47 proteins; and (iii) although simultaneous fits of 5 K absorption, emission, nonresonant holes, and RT CD spectra provide reasonable fits when Chl24, Chl26, or Chl29 contributes the most to the lowest energy exciton state, it cannot be excluded that the best candidate might be Chl29, as also suggested in Refs. 10, 11, 38, 47, and 48. The latter suggestion is based on fits of the optical spectra simulated in this article. If new CD and CPL spectra are obtained for destabilized and, in particular, intact, isolated CP47, new simultaneous fits should be completed, as the positive feature near 692–693 nm (if present, vide supra) could change the identity of low-energy pigments as mentioned above. For example, Chl11 and Chl14, based on simple Monte Carlo simulations reported in Ref. 7 (see Fig. 3), could also contribute to the lowest energy state.

We suggest that in order to obtain a final set of parameters, which can describe both the excitonic structure and dynamics of CP47 complexes, all laboratories should use stringent analytical tools to characterize the quality of extracted complexes. Standards for low-temperature spectra have to be established, and such spectra should be routinely shown in publications or supporting/supplementary information for easy comparison. In addition, various experimental techniques should be applied to samples from the same batch. For example, it is not advisable to simultaneously fit spectra from various publications, as sometimes done in the literature. If the complexes measured in different laboratories at 77 and 5 K constituted different mixtures, one set of parameters will never simultaneously describe both sets of data (see Supplementary Fig. 6 and the corresponding discussion above). Regarding time-domain data, it is often not clear to what extent the samples were composed from a mixture of intact and destabilized complexes, as low-temperature absorption and emission spectra are not reported. Finally, in light of the data and simulation studies for CP47 complexes discussed in this work, it appears that the modeling of data obtained for the entire PSII core[11] may be even less reliable, as the site energies of CP43 and RC pigments are also not well established. Nevertheless, modeling and optical spectra for PSII core (and its components) should continue as proper assignment of pigment site energies is critical to their function.

Acknowledgments

RJ and VZ acknowledge useful discussions over the years with Dr. Michael Seibert (NREL), Dr. Rafael Picorel (CSIC), and Dr. E. Krausz (Australian National University).

Author Contributions

Designed the modeling studies: RJ, TR, JC, and AK. Analyzed the data: TR, AK, MJ, and RJ. Wrote the first draft of the article: RJ. Contributed to the writing of the article: AK, KCR, MJ, and VZ. Made the critical revisions and approved the final version: RJ. All authors reviewed and approved the final article as well.

Supplementary Materials

Supplementary figure 1. Spectral fits for Model 24B.

Supplementary figure 2. Spectral fits for Model 26B.

Supplementary figure 3. Spectral fits for Model 29B.

Supplementary figure 4. Simulated spectra for Model 29AM.

Supplementary figure 5. Simulated spectra for Model 29BM.

Supplementary figure 6. Simulated spectra for Model 29CPM.

Supplementary table 1. Comparison of CP47 site energies of Renger and coworkers.

Supplementary table 2. TrEsp electronic coupling constants used in this work.

Supplementary table 3. Poisson-TrEsp electronic coupling constants used by Shibata et al.

REFERENCES

1. Blankenship RE. *Molecular Mechanism of Photosynthesis*. Oxford: Blackwell Science; 2002.
2. May V, Kühn O. Charge and Energy Transfer Dynamics in Molecular Systems. Berlin: Wiley-VCH; 2000.
3. Kell A, Feng X, Reppert M, Jankowiak R. On the shape of the phonon spectral density in photosynthetic complexes. *J Phys Chem B*. 2013;117:7317–7323.
4. Rätsep M, Freiberg A. Electron–phonon and vibronic couplings in the FMO bacteriochlorophyll *a* antenna complex studied by difference fluorescence line narrowing. *J Lumin*. 2007;127:251–259.
5. Rätsep M, Pieper J, Irrgang K-D, Freiberg A. Excitation wavelength-dependent electron–phonon and electron–vibrational coupling in the CP29 antenna complex of green plants. *J Phys Chem B*. 2008;112:110–118.
6. Pieper J, Rätsep M, Schmitt F-J, et al. Excitonic energy level structure and pigment–protein interactions in the recombinant water-soluble chlorophyll protein. I. difference fluorescence line-narrowing. *J Phys Chem B*. 2011;115:4042–4052.
7. Reppert M, Acharya K, Neupane B, Jankowiak R. Lowest electronic states of the CP47 antenna protein complex of photosystem II: simulation of optical spectra and revised structural assignments. *J Phys Chem B*. 2010;114:11884–11898.
8. Dang NC, Zazubovich Z, Reppert M, et al. The CP43 proximal antenna complex of higher plant photosystem II revisited: modeling and hole burning study I. *J Phys Chem B*. 2008;112:9921–9933.
9. Adolphs J, Müh F, Madjet ME-A, Renger T. Calculation of pigment transition energies in the FMO protein. *Photosynth Res*. 2008;95:197–209.
10. Raszewski G, Renger T. Light harvesting in photosystem II core complexes is limited by the transfer to the trap: can the core complex turn into a photoprotective mode? *J Am Chem Soc*. 2008;130:4431–4446.
11. Shibata Y, Nishi S, Kawakami K, Shen J-R, Renger T. Photosystem II does not possess a simple excitation energy funnel: time-resolved fluorescence spectroscopy meets theory. *J Am Chem Soc*. 2013;135:6903–6914.
12. Müh F, Madjet ME-A, Adolphs J, et al. α-helices direct excitation energy flow in the Fenna–Matthews–Olson protein. *Proc Natl Acad Sci U S A*. 2007;104:16862–16867.
13. Damjanović A, Kosztin I, Kleinekathöfer U, Schulten K. Excitons in a photosynthetic light-harvesting system: a combined molecular dynamics, quantum chemistry, and polaron model study. *Phys Rev E*. 2002;65:031919.
14. Gao J, Shi W-J, Ye J, et al. QM/MM modelling of environmental effects on electronic transitions of the FMO complex. *J Phys Chem B*. 2013;117:3488–3495.
15. Cole DJ, Chin AW, Hine NDM, Haynes PD, Payne MC. Toward Ab initio optical spectroscopy of the Fenna–Matthews–Olson complex. *J Phys Chem Lett*. 2013;4:4206–4212.
16. Jankowiak R, Reppert M, Zazubovich V, Pieper J, Reinot T. Site selective and single complex laser-based spectroscopies: a window on excited state electronic structure, excitation energy transfer, and electron–phonon coupling of selected photosynthetic complexes. *Chem Rev*. 2011;111:4546–4598.
17. Jankowiak R. Probing electron-transfer times in photosynthetic reaction centers by hole-burning spectroscopy. *J Phys Chem Lett*. 2012;3:1684–1694.
18. Hofmann C, Ketelaars M, Matsushita M, Michel H, Aartsma TJ, Köhler J. Single-molecule study of the electronic couplings in a circular array of molecules: light-harvesting-2 complex from *Rhodospirillum molischianum*. *Phys Rev Lett*. 2003; 90:013004.
19. Berlin Y, Burin A, Friedrich J, Köhler J. Low temperature spectroscopy of proteins. Part II: experiments with single protein complexes. *Phys Life Rev*. 2007;4: 64–89.
20. Garab G, van Amerongen H. Linear dichroism and circular dichroism in photosynthesis research. *Photosynth Res*. 2009;101:135–146.
21. Steinberg IZ. Circular polarization of luminescence: biochemical and biophysical applications. *Annu Rev Biophys Bioeng*. 1978;7:113–137.
22. Barzda V, Mustárdy L, Garab G. Size dependency of circular dichroism in macroaggregates of photosynthetic pigment–protein complexes. *Biochemistry*. 1994; 33:10837–10841.
23. Gussakovsky EE, Shahak Y, van Amerongen H, Barzda V. Circularly polarized chlorophyll luminescence reflects the macro-organization of grana in pea chloroplasts. *Photosynth Res*. 2000;65:83–92.
24. Hall J, Renger T, Picorel R, Krausz E. Circularly polarized luminescence spectroscopy reveals low-energy excited states and dynamic localization of vibronic transitions in CP43. *Biochim Biophys Acta*. 2016;1857:115–128.
25. Chauvet A, Jankowiak R, Kell A, Picorel R, Savikhin S. Does the singlet minus triplet spectrum with major photobleaching band near 680–682 nm represent an intact reaction center of photosystem II? *J Phys Chem B*. 2015;119:448–455.
26. Groot M-L, Peterman EJG, van Stokkum IHM, Dekker JP, van Grondelle R. Triplet and fluorescing states of the CP47 antenna complex of photosystem II studied as a function of temperature. *Biophys J*. 1995;68:281–290.
27. de Weerd FL, van Stokkum IH, van Amerongen H, Dekker JP, van Grondelle R. Pathways for energy transfer in the core light-harvesting complexes CP43 and CP47 of photosystem II. *Biophys J*. 2002;82:1586–1597.
28. Cho M. Coherent two-dimensional optical spectroscopy. *Chem Rev*. 2008;108: 1331–1418.
29. Abramavicius D, Palmieri B, Voronine DV, Šanda F, Mukamel S. Coherent multidimensional optical spectroscopy of excitons in molecular aggregates; quasiparticle versus supermolecule perspectives. *Chem Rev*. 2009;109:2350–2408.
30. Reimers JR, Biczysko M, Bruce D, et al. Challenges facing an understanding of the nature of low-energy excited states in photosynthesis. *Biochim Biophys Acta*. 2016. [Submitted].
31. Grozdanov D, Herascu N, Reinot T, Jankowiak R, Zazubovich V. Low-temperature protein dynamics of the B800 molecules in the LH2 light-harvesting complex: spectral hole burning study and comparison with single photosynthetic complex spectroscopy. *J Phys Chem B*. 2010;114:3426–3438.
32. Herascu N, Ahmouda S, Picorel R, et al. Effects of the distributions of energy or charge transfer rates on spectral hole burning in pigment–protein complexes at low temperatures. *J Phys Chem B*. 2011;115:15098–15109.
33. Rancova O, Jankowiak R, Kell A, Jassas M, Abramavicius D. Band structure of the *Rhodobacter sphaeroides* photosynthetic reaction center from simulations of low temperature absorption and transient hole-burned spectra. *J Phys Chem B*. 2016. [Submitted].
34. Picorel R, Alfonso M, Seibert M. Isolation of CP43 and CP47 photosystem II proximal antenna complexes from plants. In: Walker JM, ed. *Methods in Molecular Biology*. Vol 274. Totowa, NJ: Humana; 2004:129–135.
35. Picorel R, Alfonso M, Seibert M. Isolation and purification of CP43 and CP47 photosystem II proximal antenna complexes from plants. In: Walker JM, ed. *Methods in Molecular Biology*. Vol 684. New York: Springer; 2011:105–112.
36. Neupane B, Dang NC, Acharya A, et al. Insight into the electronic structure of the CP47 antenna protein complex of photosystem II: hole burning and fluorescence study. *J Am Chem Soc*. 2010;132:4214–4229.
37. Acharya K, Neupane B, Reppert M, Feng X, Jankowiak R. On the unusual temperature-dependent emission of the CP47 antenna protein complex of photosystem II. *J Phys Chem Lett*. 2010;1:2310–2315.
38. D'Haene SE, Sobotka R, Bučinská L, Dekker JP, Komenda J. Interaction of the PsbH subunit with a chlorophyll bound to histidine 114 of CP47 is responsible for the red 77 K fluorescence of photosystem II. *Biochim Biophys Acta*. 2015; 1847:1327–1334.
39. Chen J, Kell A, Acharya K, Kupitz C, Fromme P, Jankowiak R. Critical assessment of the emission spectra of various photosystem II core complexes. *Photosynth Res*. 2015;124:253–265.
40. Umena Y, Kawakami K, Shen J-R, Kamiya N. Crystal structure of oxygen-evolving photosystem II at a resolution of 1.9 Å. *Nature*. 2011;473:55–60.
41. Krausz E, Hughes JL, Smith PJ, Pace RJ, Arsköld SP. Assignment of the low-temperature fluorescence in oxygen-evolving photosystem II. *Photosynth Res*. 2005;84:193–199.
42. de Weerd FL, Palacios MA, Andrizhiyevskaya EG, Dekker JP, van Grondelle R. Identifying the lowest electronic states of the chlorophylls in the CP47 core antenna protein of photosystem II. *Biochemistry*. 2002;41:15224–15233.
43. Chen H, Wang L, Qu Y, et al. Investigation of guanidine hydrochloride induced chlorophyll protein 43 and 47 denaturation in the terahertz frequency range. *J Appl Phys*. 2007;102:074701.
44. Groot ML, Breton J, van Wilderen LJGW, Dekker JP, van Grondelle R. Femtosecond visible/visible and visible/mid-IR pump-probe study of the photosystem II core antenna complex CP47. *J Phys Chem B*. 2004;108:8001–8006.
45. Masters V, Smith P, Krausz E, Pace R. Stark shifts and exciton coupling in PSII 'supercores'. *J Lumin*. 2001;9(4–95):267–270.
46. Wang J, Gosztola D, Ruffle SV, et al. Functional asymmetry of photosystem II D1 and D2 peripheral chlorophyll mutants of *Chlamydomonas reinhardtii*. *Proc Natl Acad Sci U S A*. 2002;99:4091–4096.
47. Polívka T, Kroh P, Pšenčík J, et al. Hole-burning study of excited energy transfer in the antenna protein CP47 of *Synechocystis* sp. PCC 6803 mutant H114Q. *J Lumin*. 1997;7(2–74):600–602.
48. Shen G, Vermaas WFJ. Mutation of chlorophyll ligands in the chlorophyll-binding CP47 protein as studied in a *Synechocystis* sp. PCC 6803 photosystem I-less background. *Biochemistry*. 1994;33:7379–7388.
49. Loll B, Kern J, Saenger W, Zouni A, Biesiadka J. Towards complete cofactor arrangement in the 3.0 Å resolution structure of photosystem II. *Nature*. 2005; 438:1040–1044.
50. Müh F, Renger T, Zouni A. Crystal structure of cyanobacterial photosystem II at 3.0 Å resolution: a closer look at the antenna system and the small membrane-intrinsic subunits. *Plant Physiol Biochem*. 2008;46:238–264.

51. Renge I, Mauring K. Spectral shift mechanisms of chlorophylls in liquids and proteins. *Spectrochim Acta A*. 2013;102:301–313.
52. Renger T, Marcus RA. On the relation of protein dynamics and exciton relaxation in pigment–protein complexes: an estimation of the spectral density and a theory for the calculation of optical spectra. *J Chem Phys*. 2002;116:9997–10019.
53. Alfonso M, Montoya G, Cases R, Rodríguez R, Picorel R. Core antenna complexes, CP43 and CP47, of higher plant photosystem II. spectral properties, pigment stoichiometry, and amino acid composition. *Biochemistry*. 1994;33:10494–10500.
54. Nelder JA, Mead R. A simplex method for function minimization. *Comput J*. 1965;7:308–313.
55. Madjet ME, Abdurahman A, Renger T. Intermolecular coulomb couplings from ab initio electrostatic potentials: application to optical transitions of strongly coupled pigments in photosynthetic antennae and reaction centers. *J Phys Chem B*. 2006;110:17268–17281.
56. Mohamed A, Nagao R, Noguchi T, Fukumura H, Shibata Y. Structure-based modelling of fluorescence kinetics of photosystem II: relation between its dimeric form and photoregulation. *J Phys Chem B*. 2016;120:365–376.
57. Guskov A, Kern J, Gabdulkhakov A, et al. Cyanobacterial photosystem II at 2.9-Å resolution and the role of quinones, lipids, channels and chloride. *Nat Struct Mol Biol*. 2009;16:334–342.
58. den Hartog FTH, Dekker JP, van Grondelle S. Spectral distributions of "trap" pigments in the RC, CP47, and CP47–RC complexes of photosystem II at low temperature: a fluorescence line-narrowing and hole-burning study. *J Phys Chem B*. 1998;102:11007–11016.
59. Krausz E, Hughes JL, Smith P, Pace R, Peterson Årsköld S. Oxygen-evolving photosystem II core complexes: a new paradigm based on the spectral identification of the charge-separating state, the primary acceptor and assignment of low-temperature fluorescence. *Photochem Photobiol Sci*. 2005;4:744–753.
60. Olbrich C, Strümpfer J, Schulten K, Kleinekathöfer U. Theory and simulation of the environmental effects on FMO electronic transitions. *J Phys Chem Lett*. 2011;2:1771–1776.
61. Rivera E, Montemayer D, Masia M, Coker DF. Influence of site-dependent pigment–protein interactions on excitation energy transfer in photosynthetic light harvesting. *J Phys Chem B*. 2013;117:5510–5521.
62. Chandrasekaran S, Aghtar M, Valleau S, Aspuru-Guzik A, Kleinekathöfer U. Influence of force fields and quantum chemistry approach on spectral densities of BChl *a* in solution and in FMO proteins. *J Phys Chem B*. 2015;119:9995–10004.